A novel decoupling technique for multiple-row microstrip transceiver array designs

Xinqiang Yan[1,2], Long Wei[2], Rong Xue[1], and Xiaoliang Zhang[3]

[1]*State Key Laboratory of Brain and Cognitive Science, Beijing MRI Center for Brain Research, Institute of Biophysics, Chinese Academy of Sciences, Beijing, Beijing, China,* [2]*Key Laboratory of Nuclear Analysis Techniques, Institute of High Energy Physics, Chinese Academy of Sciences, Beijing, Beijing, China,* [3]*Department of Radiology and Biomedical Imaging, University of California San Francisco and UCSF/UC Berkeley Joint Graduate Group in Bioengineering, San Francisco, California, United States*

INTRODUCTION: Compared with single-row transceiver coil arrays, multiple-row arrays exhibit larger imaging coverage and the capability of parallel imaging and parallel excitation (pTx) along z-direction [1, 2]. With the advantages of low mutual coupling, simple structure and less radiative loss, microstrip transceiver arrays have been widely used in ultrahigh field MRI [3-5]. To enlarge the imaging coverage, multiple-row microstrip array design seems necessary. However, reducing the strong coupling between elements of adjacent rows is technologically challenging. In this study, we proposed a novel decoupling technique based on the ICE decoupling method to reduce the strong coupling of elements from adjacent rows. The feasibility and performance of this novel decoupling technique were validated and investigated through bench tests and MR imaging experiments.

MATERIALS and METHODS: ICE decoupling method have been successfully applied to reduce the coupling between adjacent coil elements by inserting a decoupling element [6, 7]. It has been demonstrated that the mutual coupling between the coil element and decoupling element (X_{cd}) has to satisfy a condition to achieve good decoupling performance [6]. However, the space between two microstrip resonators from adjacent rows is very limited and thus it is difficult to insert a decoupling element which can meet the condition. To address this problem, the decoupling element was closely placed next to the coil elements rather than inserted between them.

Two microstrip elements were arranged in different rows, as shown in Figure 1. Each element using Teflon has a length of 9 cm and a thickness of 1.5 cm The widths of ground and stripe conductor were 4.5 cm and 1 cm, respectively. The distance between the two elements was 1 cm. For each microstrip element, a trimmer capacitor C_{t1} was terminated at the feed end for tuning and a fixed capacitor C_{t2} (33pF, ATC Corp, Huntington Station, NY) was terminated at the other end. To avoid the condition that the value of the matching capacitor was too small, a 1.5 pF fixed capacitor and a trimmer capacitor C_m connected in shunt were used for matching [8]. A resonator with two capacitors (C_{d1} and C_{d2}) terminated at both ends and one variable capacitor (C_{dt}) terminated at the center was applied as the decoupling element. RF cable traps were placed between cable and coil element to avoid possible cable resonance. Both coils were used for transmission and reception, matching to 50 Ohm and tuning to 297.2 MHz.

Bench tests of the two elements with and without the decoupling element were performed by using an Agilent E5071C network analyzer. To assure the performance of the proposed decoupling method, a pattern comparison of MR images on a cylindrical water phantom acquired with: (1) a single coil element without the other element; (2) one coil element of the coupled 2-channel array; and (3) one coil element of the well decoupled 2-channel array; was performed using a gradient echo (GRE) sequence with the identical parameters. The parameters of the GRE sequence used were: FA=25 degree, TR/TE=100/10 ms, FOV=210×210 mm^2, matrix= 256×256, slice thickness= 3 mm. During the experiment, the cylindrical phantom (length 37 cm; diameter 16 cm; σ = 0.59 S/m; ε_r = 78) was placed 3 cm below the coil arrays. MR imaging data were acquired on a 7T whole-body scanner (Siemens, Erlangen, Germany).

RESULTS AND DISCUSSIONS: Figures 2a and 2b show the S_{11} and S_{21} plots of the two microstrip elements without decoupling treatments. It is clear that the two elements were strongly coupled (S_{21}=-7.9 dB) and the resonant peak was obviously split. By using the novel decoupling method, the isolation was improved to -25.3 dB and no resonant peak splitting was observed (Figures 2c and 2d). These results indicated the two coupled elements from adjacent rows could be decoupled sufficiently by the proposed decoupling method.

Figure 3 shows the water phantom images acquired from (a) individual elements, (b) elements from the coupled array and (c) elements from the decoupled array. The strong electromagnetic coupling, indicated by S-parameter results shown above, could also be validated by Figure 3b that part of the MR signals was obviously transferred to the other coil element. Whereas the MR images from the decoupled array (Figure 3c) have a similar patterns compared with the images from the individual elements, indicating that the proposed decoupling method could effectively reduce the strong coupling to a sufficient small value.

CONCLUSION: Both bench test and MR imaging results showed that the proposed novel decoupling technique could reduce the strong coupling between microstrip elements from adjacent rows. This design is easy to be fabricated in practice, and very suitable for designing multiple-row parallel arrays with large channel counts at ultrahigh fields.

REFERENCES [1] N. I. Avdievich, Appl. MR, vol. 41, pp. 483-506, 2011. [2] G. Shajan, et al, MRM, vol.71, pp. 870-879, 2014. [3] G. Adriany, et al, MRM, vol. 53, pp.434-445, 2005. [4] D. O. Brunner, et al, Proc. ISMRM, p. 448, 2007. [5] B. Wu, et al, MRM, vol. 68, pp. 1332-1338, 2012. [6] Y. Li, et al, Med. Phys., vol. 38, pp. 4086-4093, 2011. [7] X. Yan, et al, IEEE Trans. Med. Imaging, vol. 33, pp. 1781-178, 2014. [8] G. Shajan, et al, MRM, vol. 66, pp. 596-604, 2011.

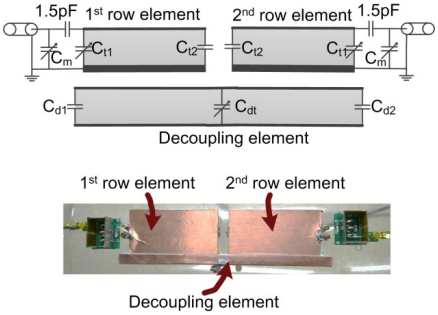

Figure 1 Equivalent circuit (top) and photograph (bottom) of the double-row transmission line array with a decoupling element.

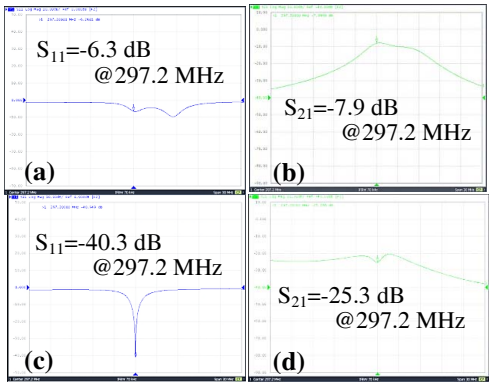

Figure 2 (a) S_{11} plot without decoupling element. **(b)** S_{21} plot without the decoupling element. **(c)** S_{11} plot with the decoupling element. **(d)** S_{21} plot with the decoupling element.

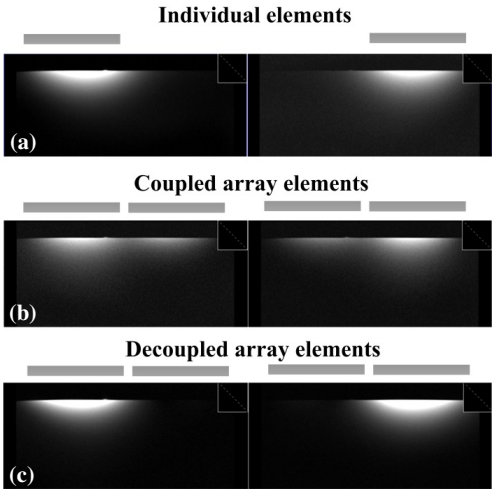

Figure 3 Water phantom images in the sagittal plane acquired from **(a)** individual elements, **(b)** elements from the coupled array (-7.9 dB) and **(c)** elements from the ICE-decoupled array (-25.3 dB).